Sound & Vibration
DOI:10.32604/sv.2020.08469
Article

Position and Velocity Time Delay for Suppression Vibrations of a Hybrid Rayleigh-Van der Pol-Duffing Oscillator

Y. A. Amer[1], A. T. El-Sayed[2] and M. N. Abd El-Salam[3,*]

[1]Mathematics Department, Science Faculty, Zagazig University, Zagazig, Egypt
[2]Basic Sciences Department, Modern Academy for Engineering and Technology, Cairo, Egypt
[3]Basic Sciences Department, Higher Technological Institute, 10th of Ramadan City, Egypt
[*]Corresponding Author: M. N. Abd EL-Salam. Email: mansour.naserallah@yahoo.com
Received: 28 August 2019; Accepted: 15 May 2020

Abstract: In this paper, we used time delay feedback to minimize the vibrations of a hybrid Rayleigh–van der Pol–Duffing oscillator. This system is a one-degree-of-freedom containing the cubic and fifth nonlinear terms and an external force. We applied the multiple scales method to get the solution from first approximation. Graphically and numerically, we studied the system before and after adding time delay feedback at the primary resonance case ($\Omega \cong \omega$). We used MATLAB program to simulate the efficacy of different parameters and the time delay on the main system.

Keywords: Position time delay feedback; velocity time delay feedback; multiple scales method; resonance cases

1 Introduction

The Duffing oscillator is used as a main type model for different engineering and physical problems such that electric circuit, oscillation of plasma, optical stability and the buckled beam [1–6]. Wen et al. [7] presented two kinds of Van der Pol oscillator containing fractional order terms. The averaging method used for obtaining the approximation solution. The additional stiffness coefficient is almost zero and the additional damping coefficient damping is almost the maximum value when the two kinds of Van der Pol fractional existed. The vibrations of Van der Pol oscillator are suppressed by using the nonlinear time delayed feedback controller and the effectiveness of the feedback gain on bifurcation point is studied numerically [8]. In [9], the dynamic stable and unstable behavior of the ring of coupled Van der Pol oscillators are discussed numerically also, the amplitude of the oscillator increased if the stability conditions are not satisfied. The Homotopy analysis method is used to obtain the analytically solution for the first time of a single–well, double–well and double–hump van der pol–Duffing oscillator [10]. Soleman et al. [11], utilized the position time delayed feedback control to restrain the auto parametric dynamical system vibrations. The Rayleigh equation with a cubic nonlinearity oscillator is presented in [12] and is studied for the following cases: positive linear and cubic coefficients, positive linear and negative cubic coefficients and negative linear and positive cubic coefficients. [13–15], modified and studied the bifurcation of Van der Pol–Duffing–Rayleigh oscillator. Of great importance to restrained the vibrations of Van der Pol oscillator. One of the important kinds of controllers is the time delay control.

The time delay control is used for suppression the nonlinear beam vibrations in [16] and they deduced that, the vibrations could be reduced for some values of time delay, which called the vibration suppression region. The positive position feedback controller is adjusted with the time delay to minimize the horizontal vibration of a magnetically levitated body and to control the vibration of a forced and self-exited nonlinear beam [17,18]. The time delay control is used to suppress the vibrations of many dynamical systems such that, Stainless-steel beam, Helicopter blade flapping and Duffing oscillator [19–21]. In this article, the vibrations of a hybrid Rayleigh–Van der Pol–Duffing oscillator exciting by external forces are suppressed by using position and velocity time delay feedback controllers. Numerically, we simulated the behavior of the system without and with time delay controllers. We used MATLAB program to simulate the efficacy of different parameters and the time delay on the main system. The influences of some chosen coefficients are illustrated numerically and analytically. The rapprochement between numeric and analytic solution is offered.

2 Mathematical Formulation

The one-degree-of-freedom of a hybrid Rayleigh–Van der Pol–Duffing oscillator presented in [15] as:

$$\ddot{u} - 2\mu\omega\dot{u}(1 - \frac{\eta}{\omega}\dot{u} - \beta u^2 - \frac{\delta}{\omega^2}\dot{u}^2 - \frac{\theta}{\omega}\dot{u}u^2) + 2\mu\omega^2u^3(k + \lambda u^2) + \omega^2 u = 0 \tag{1}$$

We used the position and velocity time delay to minimize the vibrations of a hybrid Rayleigh–Van der Pol–Duffing oscillator subjected to an external force as the following:

$$\begin{aligned} &\ddot{u} - 2\varepsilon\hat{\mu}\omega\dot{u}(1 - \frac{\eta}{\omega}\dot{u} - \beta u^2 - \frac{\delta}{\omega^2}\dot{u}^2 - \frac{\theta}{\omega}\dot{u}u^2) + 2\varepsilon\hat{\mu}\omega^2u^3(k + \lambda u^2) + \omega^2 u \\ &= \varepsilon\hat{f}\cos(\Omega t) - \varepsilon(\hat{\gamma}_1 u(t-\tau_1) + \hat{\gamma}_2\dot{u}(t-\tau_2)) \end{aligned} \tag{2}$$

where, $\hat{\mu} = \frac{\mu}{\varepsilon}, \hat{f} = \frac{f}{\varepsilon}, \hat{\gamma}_1 = \frac{\gamma_1}{\varepsilon}, \hat{\gamma}_2 = \frac{\gamma_2}{\varepsilon}$ and the displacement of van der pol oscillator is u. The nonlinearities coefficients are η, β, δ, θ, k and λ. The natural frequency of Van der Pol oscillator is ω. The excitation's amplitude and frequency are f and Ω. μ, is the damping coefficient. The time delay feedback signals are γ_1 and γ_2.

2.1 Perturbation Analysis

We used the multiple scales method [22,23] to obtain the solutions of Eq. (2) up to the first approximation:

$$u(t;\varepsilon) = u_0(T_0, T_1) + \varepsilon u_1(T_0, T_1) \tag{3}$$

The first and second derivatives take the forms:

$$\frac{d}{dt} = D_0 + \varepsilon D_1 + \ldots \tag{4}$$

$$\frac{d^2}{dt^2} = D_0^2 + 2\varepsilon D_0 D_1 + \ldots \tag{5}$$

For the first approximation solution, we performed a two time scales $T_r = \varepsilon^r t$ such that $(\mathrm{r} = 0, 1)$. The derivatives $D_r = \frac{\partial}{\partial T_r}(\mathrm{r} = 0, 1)$. Inserting Eqs. (3)–(5) in Eq. (2) and equating the coefficients of the same power of ε.

$O(\varepsilon^0)$:

$$(D_0^2+\omega^2)u_0=0 \tag{6}$$

$O(\varepsilon)$:

$$\begin{aligned}(D_0^2+\omega^2)u_1 &= -2D_0D_1u_0+2\hat{\mu}\omega D_0u_0-2\hat{\mu}\eta(D_0u_0)^2-2\hat{\mu}\omega\beta(D_0u_0)u_0^2-\frac{2\hat{\mu}\delta}{\omega}(D_0u_0)^3\\ &\quad -2\hat{\mu}\theta(D_0u_0)^2u_0^2-2\hat{\mu}k\omega^2u_0^3-2\hat{\mu}\lambda\omega^2u_0^5-\hat{\gamma}_1u_{0\tau_1}-\hat{\gamma}_2D_0u_{0\tau_2}+\hat{f}\cos\Omega t\end{aligned} \tag{7}$$

Eq. (6) is a homogenous differential equation of second order its solution takes the form:

$$u_0(\mathrm{T}_0,\mathrm{T}_1)=A(T_1)e^{(i\omega T_0)}+c.c \tag{8}$$

Denote that A is a complex function in T_1. The complex conjugate parts collected in the term c.c. From Eq. (8), we have

$$u_{0\tau_1}(\mathrm{T}_0,\mathrm{T}_1)=A_{\tau_1}(T_1)e^{i\omega(T_0-\tau_1)}+c.c \tag{9}$$

$$D_0u_{0\tau_2}(T_0,T_1)=i\omega A_{\tau_2}(T_1)e^{i\omega(T_0-\tau_2)}+c.c \tag{10}$$

By using Taylor expansion, we get the following form of A_{τ_1} and A_{τ_2}:

$$A_{\tau_1}(\mathrm{T}_1)=\mathrm{A}(\mathrm{T}_1-\varepsilon\tau_1)\cong A(T_1)-\varepsilon\tau_1D_1A+O(\varepsilon^2) \tag{11}$$

$$A_{\tau_2}(\mathrm{T}_1)=\mathrm{A}(\mathrm{T}_1-\varepsilon\tau_2)\cong A(\mathrm{T}_1)-\varepsilon\tau_2D_1A+O(\varepsilon^2) \tag{12}$$

For computation the right hand sides of Eq. (7), we will use Eqs. (8)–(10) so that,

$$\begin{aligned}(D_0^2+\omega^2)\mathrm{u}_1 &= \Big(-2i\omega D_1A+2i\hat{\mu}\omega^2A-2i\hat{\mu}\omega^2(\beta+3\delta)A^2\bar{A}-6\hat{\mu}\omega^2KA^2\bar{A}-20\hat{\mu}\lambda\omega^2\mathrm{A}^3\bar{\mathrm{A}}^2\\ &\quad -(\hat{\gamma}_1\mathrm{A}_{\tau_1}e^{-i\omega\tau_1}+i\omega\hat{\gamma}_2\mathrm{A}_{\tau_2}e^{-i\omega\tau_2})\Big)e^{i\omega T_0}+\Big(2\hat{\mu}\eta\omega^2A^2\Big)e^{2i\omega T_0}+\Big(-2\hat{\mu}\omega^2\mathrm{A}^3((\mathrm{k}+5\lambda\mathrm{A}\bar{\mathrm{A}})\\ &\quad +i(\beta+\delta))\Big)e^{3i\omega T_0}+\Big(2\hat{\mu}\theta\omega^2\mathrm{A}^4\Big)e^{4i\omega T_0}-\Big(2\hat{\mu}\lambda\omega^2\mathrm{A}^5\Big)e^{5i\omega T_0}+\left(\frac{\hat{f}}{2}\right)\mathrm{e}^{i\Omega T_0}+c.c\end{aligned} \tag{13}$$

For the particular solution of Eq. (13) be bounded, we will remove the secular terms such that,

$$u_1(\mathrm{T}_0,\mathrm{T}_1)=M_1e^{2i\omega T_0}+M_2e^{3i\omega T_0}+M_3e^{4i\omega T_0}+M_4e^{5i\omega T_0}+M_5e^{i\Omega T_0}+c.c \tag{14}$$

where $M_\partial\,(\partial=1,\ldots,5)$ offering complex functions in T_1 are defined in the "Appendix". From the first approximation, there is only one resonance case, which is the Primary resonance $\Omega\cong\omega$.

3 Periodic Solutions

On this treatise, the primary resonance $(\Omega\cong\omega)$ is used to discuss the solvability conditions. We introduced a detuning parameter (σ) so that:

$$\Omega=\omega+\varepsilon\hat{\sigma}=\omega+\sigma \tag{15}$$

Including Eqs. (11), (12) & (15) into Eq. (13) for compiling the solvability conditions as:

$$\begin{aligned}&-2i\omega D_1A+(\varepsilon\tau_1\hat{\gamma}_1e^{-i\omega\tau_1})D_1A+i(\varepsilon\omega\tau_2\hat{\gamma}_2e^{-i\omega\tau_2})D_1A+2i\hat{\mu}\omega^2A-2i\hat{\mu}\omega^2(\beta+3\delta)A^2\bar{A}-6\hat{\mu}\omega^2KA^2\bar{A}\\&-20\hat{\mu}\lambda\omega^2A^3\bar{A}^2-(\hat{\gamma}_1e^{-i\omega\tau_1})A-i(\omega\hat{\gamma}_2e^{-i\omega\tau_2})A+\frac{\hat{f}}{2}e^{i\hat{\sigma}T_1}=0\end{aligned}\tag{16}$$

Exchanging $A(T_1)$ by the polar form as:

$$A=\frac{1}{2}a\,e^{i\varphi}\tag{17}$$

$$D_1A=\frac{1}{2}(a'+ia\varphi')e^{i\varphi}\tag{18}$$

where φ and a are the motion's steady state phases and amplitudes which are functions in T_1 and $()'=\frac{d}{dT_1}$. Subjoining Eqs. (17) and (18) into Eq. (16) such that:

$$\begin{aligned}&-i\omega(a'+ia\varphi')+(\frac{\varepsilon\tau_1\hat{\gamma}_1}{2}e^{-i\omega\tau_1})(a'+ia\varphi')+i(\frac{\varepsilon\omega\tau_2\hat{\gamma}_2}{2}e^{-i\omega\tau_2})(a'+ia\varphi')+i\hat{\mu}\omega^2a-\frac{1}{4}i\hat{\mu}\omega^2(\beta+3\delta)a^3\\&-\frac{3}{4}\hat{\mu}\omega^2Ka^3-\frac{5}{8}\hat{\mu}\lambda\omega^2a^5-(\frac{\hat{\gamma}_1}{2}e^{-i\omega\tau_1})a-i(\frac{\omega\hat{\gamma}_2}{2}e^{-i\omega\tau_2})a+\frac{\hat{f}}{2}e^{i\psi}=0\end{aligned}\tag{19}$$

where $\psi=\hat{\sigma}T_1-\varphi$. For any two equal complex numbers, the real and imaginary parts are equal so that:

$$\begin{aligned}&\left[-\omega-\frac{1}{2}\varepsilon\hat{\gamma}_1\tau_1\sin(\omega\tau_1)+\frac{1}{2}\varepsilon\omega\hat{\gamma}_2\tau_2\cos(\omega\tau_2)\right]a'+\left[\frac{1}{2}\varepsilon\hat{\gamma}_1\tau_1\cos(\omega\tau_1)+\frac{1}{2}\varepsilon\omega\hat{\gamma}_2\tau_2\sin(\omega\tau_2)\right]a\varphi'\\&+\left[\hat{\mu}\omega^2+\frac{1}{2}\hat{\gamma}_1\sin(\omega\tau_1)-\frac{1}{2}\omega\hat{\gamma}_2\cos(\omega\tau_2)\right]a-\left[\frac{1}{4}\hat{\mu}\omega^2(\beta+3\delta)\right]a^3=-\left[\frac{\hat{f}}{2}\sin(\psi)\right]\end{aligned}\tag{20}$$

$$\begin{aligned}&\left[\frac{1}{2}\varepsilon\hat{\gamma}_1\tau_1\cos(\omega\tau_1)+\frac{1}{2}\varepsilon\omega\hat{\gamma}_2\tau_2\sin(\omega\tau_2)\right]a'-\left[-\omega-\frac{1}{2}\varepsilon\hat{\gamma}_1\tau_1\sin(\omega\tau_1)+\frac{1}{2}\varepsilon\omega\hat{\gamma}_2\tau_2\cos(\omega\tau_2)\right]a\varphi'\\&-\left[\frac{1}{2}\hat{\gamma}_1\cos(\omega\tau_1)+\frac{1}{2}\omega\hat{\gamma}_2\sin(\omega\tau_2)\right]a-\left[\frac{3}{4}\hat{\mu}\omega^2k\right]a^3-\left[\frac{5}{8}\hat{\mu}\omega^2\lambda\right]a^5=-\left[\frac{\hat{f}}{2}\cos(\psi)\right]\end{aligned}\tag{21}$$

Back to the main system parameters, we have the following equations:

$$\begin{aligned}&\left[-\omega-\frac{1}{2}\varepsilon\hat{\gamma}_1\tau_1\sin(\omega\tau_1)+\frac{1}{2}\varepsilon\omega\hat{\gamma}_2\tau_2\cos(\omega\tau_2)\right]\dot{a}+\left[\frac{1}{2}\varepsilon\hat{\gamma}_1\tau_1\cos(\omega\tau_1)+\frac{1}{2}\varepsilon\omega\hat{\gamma}_2\tau_2\sin(\omega\tau_2)\right]a\dot{\varphi}\\&+\left[\hat{\mu}\omega^2+\frac{1}{2}\hat{\gamma}_1\sin(\omega\tau_1)-\frac{1}{2}\omega\hat{\gamma}_2\cos(\omega\tau_2)\right]a-\left[\frac{1}{4}\hat{\mu}\omega^2(\beta+3\delta)\right]a^3=-\left[\frac{\hat{f}}{2}\sin(\psi)\right]\end{aligned}\tag{22}$$

$$\begin{aligned}&\left[\frac{1}{2}\varepsilon\gamma_1\tau_1\cos(\omega\tau_1)+\frac{1}{2}\varepsilon\omega\gamma_2\tau_2\sin(\omega\tau_2)\right]\dot{a}-\left[-\omega-\frac{1}{2}\varepsilon\gamma_1\tau_1\sin(\omega\tau_1)+\frac{1}{2}\varepsilon\omega\gamma_2\tau_2\cos(\omega\tau_2)\right]a\dot{\varphi}\\&-\left[\frac{1}{2}\gamma_1\cos(\omega\tau_1)+\frac{1}{2}\omega\gamma_2\sin(\omega\tau_2)\right]a-\left[\frac{3}{4}\mu\omega^2k\right]a^3-\left[\frac{5}{8}\mu\omega^2\lambda\right]a^5=-\left[\frac{f}{2}\cos(\psi)\right]\end{aligned}\tag{23}$$

where, $a'=\frac{\dot{a}}{\varepsilon}$, $\varphi'=\frac{\dot{\varphi}}{\varepsilon}$ and $\dot{()}=\frac{d}{dt}$. Since $a\dot{\psi}=a\sigma-a\dot{\varphi}$ then, solve the Eqs. (22) and (23) to extract the values of $\dot{a}$ and $a\dot{\psi}$ as the following:

$$\dot{a} = \frac{1}{\xi}\left[\Gamma_1 a^5 + \Gamma_2 a^3 + \Gamma_3 a - \Gamma_4 \cos(\psi + \omega\tau_1) - \Gamma_5 \sin(\psi + \omega\tau_2) + \Gamma_6 \sin(\psi)\right] \tag{24}$$

$$a\dot{\psi} = -\frac{1}{\xi}\left[\Gamma_7 a^5 + \Gamma_8 a^3 + (\Gamma_9 - \sigma\xi)a - \Gamma_{10}\sin(\psi + \omega\tau_1) + \Gamma_{11}\cos(\psi + \omega\tau_2) - \Gamma_{12}\cos(\psi)\right] \tag{25}$$

where, the coefficients ξ and Γ_i, $i = 1, 2, \ldots, 12$ are defined in the "Appendix".

3.1 Fixed Point Solution

For steady-state solution, we may be find the fixed point of the Eqs. (22) and (23) by putting $\dot{a} = 0$ and $\dot{\psi} = 0$ leads to $\dot{\varphi} = \sigma$ so,

$$\begin{aligned}&\left[\mu\omega^2 + \frac{1}{2}\gamma_1(\sigma\tau_1\cos(\omega\tau_1) + \sin(\omega\tau_1)) + \frac{1}{2}\omega\gamma_2(\sigma\tau_2\sin(\omega\tau_2) - \cos(\omega\tau_2))\right]a - \left[\frac{1}{4}\mu\omega^2(\beta + 3\delta)\right]a^3\\ &= -\left[\frac{f}{2}\sin(\psi)\right]\end{aligned} \tag{26}$$

$$\begin{aligned}&\left[\omega\sigma + \frac{1}{2}\gamma_1(\sigma\tau_1\sin(\omega\tau_1) - \cos(\omega\tau_1)) - \frac{1}{2}\omega\gamma_2(\sigma\tau_2\cos(\omega\tau_2) + \sin(\omega\tau_2))\right]a - \left[\frac{3}{4}\mu\omega^2 k\right]a^3 - \left[\frac{5}{8}\mu\omega^2\lambda\right]a^5\\ &= -\left[\frac{f}{2}\cos(\psi)\right]\end{aligned} \tag{27}$$

Squaring then adding both sides of Eqs. (26) and (27) to obtain the following equation:

$$\begin{aligned}&\frac{25}{64}\left[\mu^2\omega^4\lambda^2\right]a^{10} + \frac{15}{16}\left[\mu^2\omega^4 k\lambda\right]a^8\\
&+\frac{1}{16}\begin{bmatrix}\mu^2\omega^4(9k^2 + (\beta + 3\delta)^2) - 20\mu\omega^3\lambda\sigma - 10\mu\omega^2\lambda\gamma_1(\sigma\tau_1\sin(\omega\tau_1) - \cos(\omega\tau_1))\\ +10\mu\omega^3\lambda\gamma_2(\sigma\tau_2\cos(\omega\tau_2) + \sin(\omega\tau_2))\end{bmatrix}a^6\\
&-\frac{1}{4}\begin{bmatrix}2\mu^2\omega^4(\beta + 3\delta) + 6\mu\omega^3 k\sigma + \mu\omega^2\gamma_1(\beta + 3\delta)(\sigma\tau_1\cos(\omega\tau_1) + \sin(\omega\tau_1))\\ +\mu\omega^3\gamma_2(\beta + 3\delta)(\sigma\tau_2\sin(\omega\tau_2) - \cos(\omega\tau_2)) + 3\mu\gamma_1 k\omega^2(\sigma\tau_1\sin(\omega\tau_1)\\ -\cos(\omega\tau_1)) - 3\mu\gamma_2\omega^3 k(\sigma\tau_2\cos(\omega\tau_2) + \sin(\omega\tau_2))\end{bmatrix}a^4\\
&+\frac{1}{4}\begin{bmatrix}\sigma^2(\gamma_1^2\tau_1^2 + \omega^2\gamma_2^2\tau_2^2) + \omega^2(4\sigma^2 + 4\mu^2 + \gamma_1^2) + 4\omega\gamma_1(\sigma^2\tau_1 + \mu\omega)\sin(\omega\tau_1)\\ -4\omega\sigma\gamma_1(1 - \mu\omega\tau_1)\cos(\omega\tau_1) - 4\omega^2\sigma\gamma_2(1 - \mu\omega\tau_2)\sin(\omega\tau_2) - 4\omega^2\gamma_2(\sigma^2\tau_2 + \mu\omega)\cos(\omega\tau_2)\\ +2\omega\gamma_1\gamma_2(\tau_2 - \tau_1)\cos(\omega\tau_1 - \omega\tau_2) - 2\omega\gamma_1\gamma_2(1 + \sigma^2\tau_2\tau_1)\sin(\omega\tau_1 - \omega\tau_2)\end{bmatrix}a^2\\
&-\left[\frac{f^2}{4}\right] = 0\end{aligned} \tag{28}$$

3.2 Equilibrium Solution of a Fixed Point

While in movement to evolve the steady state solution's stability, start with the following procedures:

$$\left.\begin{array}{l}a = a_0 + a_1\,,\ \psi = \psi_0 + \psi_1\\ \dot{a} = \dot{a}_1\,,\ \dot{\psi} = \dot{\psi}_1\end{array}\right\} \tag{29}$$

Inserting Eq. (29) into Eqs. (24) and (25) then, we obtained the following system:

$$\dot{a}_1 = \left[\left(\frac{1}{\xi} \right) \left(5\Gamma_1 a_0^4 + 3\Gamma_2 a_0^2 + \Gamma_3 \right) \right] a_1 + \left[\left(\frac{1}{\xi} \right) \left(\Gamma_4 \sin(\psi_0 + \omega\tau_1) - \Gamma_5 \cos(\psi_0 + \omega\tau_2) + \Gamma_6 \cos(\psi_0) \right) \right] \psi_1 \tag{30}$$

$$\dot{\psi}_1 = \left[\left(\frac{1}{\xi} \right) \left(5\Gamma_7 a_0^3 + 3\Gamma_8 a_0 + \frac{\Gamma_9 - \sigma\xi}{a_0} \right) \right] a_1 + \left[\left(\frac{1}{\xi a_0} \right) \left(\Gamma_{10} \cos(\psi_0 + \omega\tau_1) + \Gamma_{11} \sin(\psi_0 + \omega\tau_2) - \Gamma_{12} \sin(\psi_0) \right) \right] \psi_1 \tag{31}$$

For the above system's solution be stable, the real parts of its Eigen-values must be negative.

4 Numerical Illustration

Numerically, we applied Runge-Kutta 4th (RK-4) order method using MATLAB program to solve the differential equation of the main system after using the time delay feedback controller. This study occurs at the worst resonance case (Primary resonance) by the following values of parameters:

$$\mu = 0.01, \tau_1 = 0.03, \tau_2 = 0.05, k = 3, \eta = 1.5, \beta = 1, \delta = \frac{1}{3}, \lambda = 2, f = 0.5, \gamma_1 = 5, \gamma_2 = 2, \omega = 1$$

Fig. 1 clarifies the amplitude of the uncontrolled main system, which equal 1.5. The influence of the main system parameters (damping coefficient μ and nonlinearities coefficients $k, \eta, \beta, \delta, \lambda$ and θ) has been presented on Fig. 2. From this figure, we note that, the amplitude of the main system is monotonic decreasing in the damping coefficient μ and nonlinearities coefficients k, η, β, δ and λ but monotonic increasing in the nonlinear coefficient θ. More increasing of the damping coefficient μ leads to saturation phenomena and the amplitude value equal to 0.9 so that, the system might be need a control. After using time delay feedback controller, the main system amplitude reduced to reach 0.09 as represented on Fig. 3 this means that, the effectiveness of the controller (E_a = amplitude without control/amplitude with) equal 17.

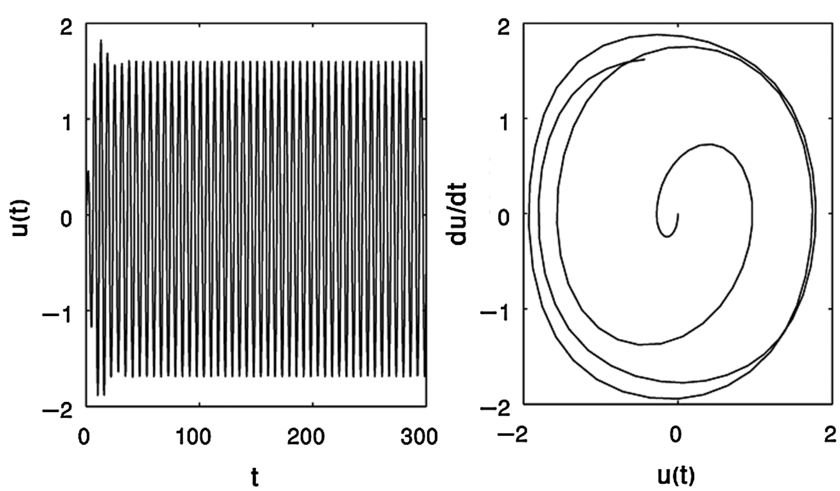

Figure 1: The time history and phase plane of uncontrolled system at primary resonance case ($\Omega \cong \omega$)

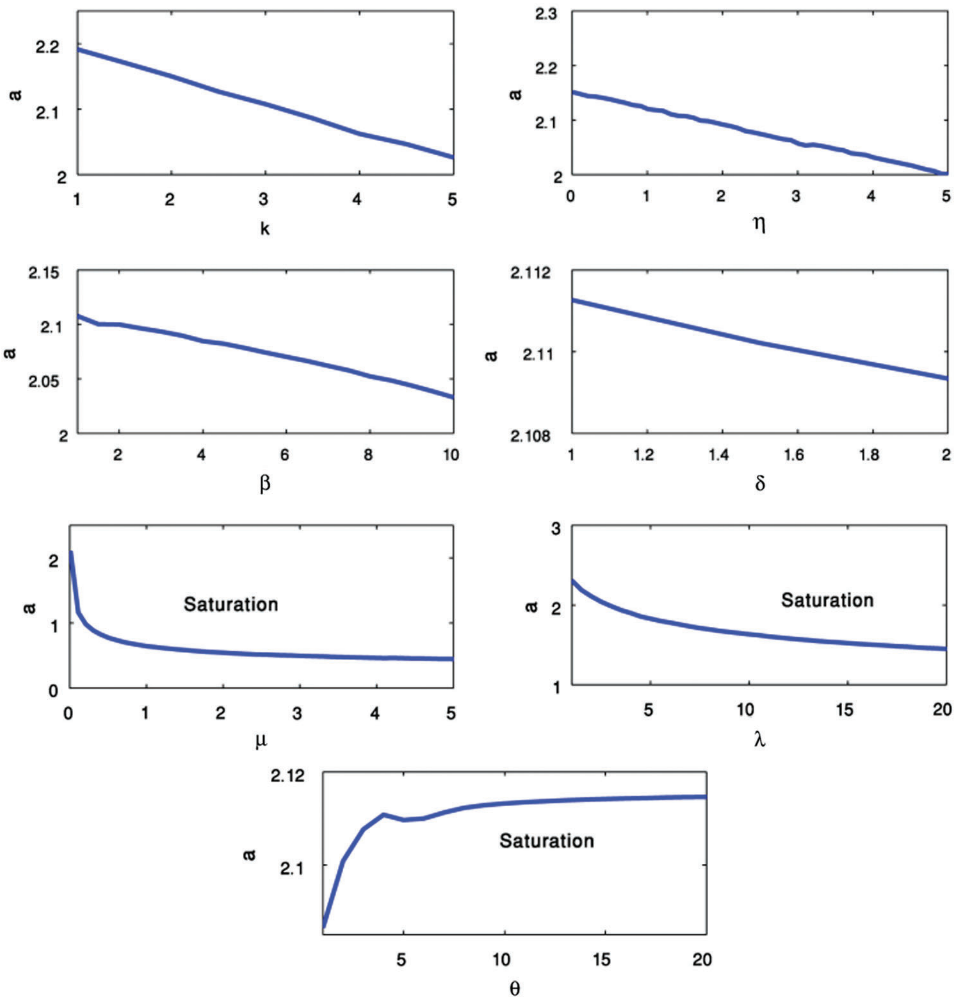

Figure 2: The influence of the parameters of the main system without control

Eq. (28) solved numerically to obtain the graphical solution for the amplitude via the detuning parameter (σ) which, presented by one peak. The response curve of the amplitude-delay τ_1 at $\tau_2 = 0$ and $\tau_2 = 0.05$ for different values of γ_1 was shown in Fig. 4. From this figure, we can see that, for small values of γ_1 the vibration suppression region (is the region at which the amplitude-delay's response curves demonstrates stable solution) increased. The response curve of the amplitude-delay τ_2 at $\tau_1 = 0$ and $\tau_1 = 0.03$ was shown in Fig. 5 for different values of γ_1. For $\tau_1 = 0$ we can notice that, the vibration suppression region increased for small values of γ_2 but at $\tau_1 = 0.03$, the vibration suppression region increased for large values of γ_2.

The response curves of the main system a against the detuning parameter σ is presented for $\tau_1 = 0.03$, $\tau_2 = 0.05$ such that the solid line expresses the stable solution of Eq. (28), while the dash one expresses the unstable solution of the same equation as shown in Fig. 6a. For large values of the external force, the main system's amplitude increase also as notice in Fig. 6b. The amplitude increasing and shift to right for small values of the time delay displacement's feedback gain γ_1 and the real part of all Eigen-Values is negative so, the solution is stable for small values of γ_1 as illustrated in Fig. 6c, and this is consistent with Fig. 4. Fig. 6d shows that, the main system's amplitude is monotonic decreasing function on the time delay velocity's feedback gains γ_2 and the solution is stable for large values of γ_2, and this is

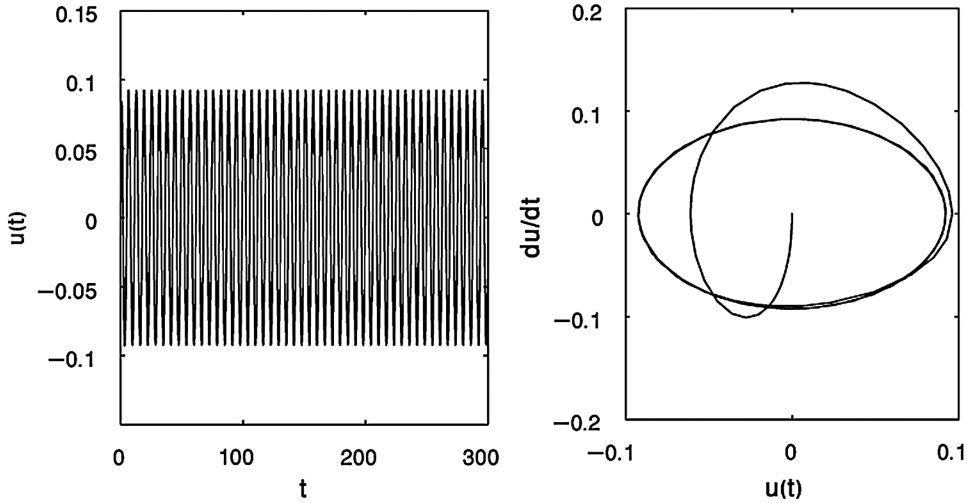

Figure 3: The time history and phase plane of controlled system at primary resonance case ($\Omega \cong \omega$)

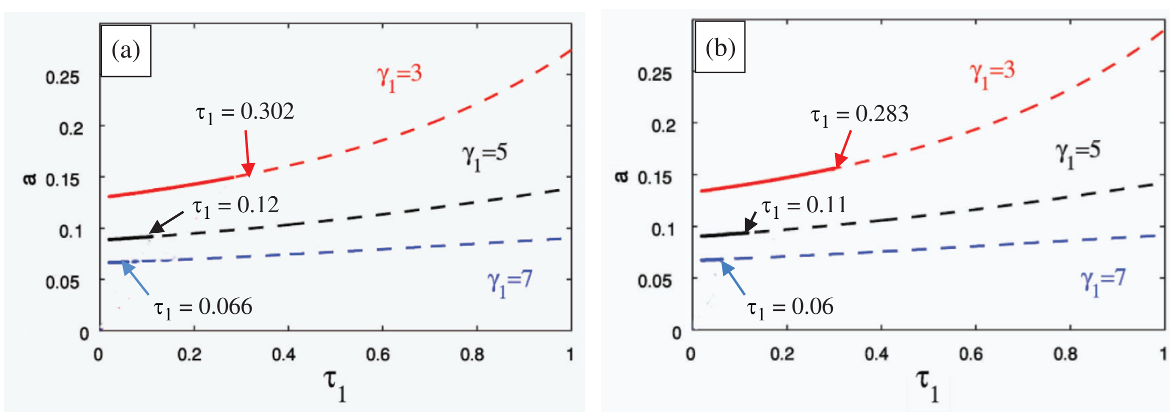

Figure 4: The response curve of the amplitude-delay τ_1 for (a) $\tau_2 = 0$ and (b) $\tau_2 = 0.05$

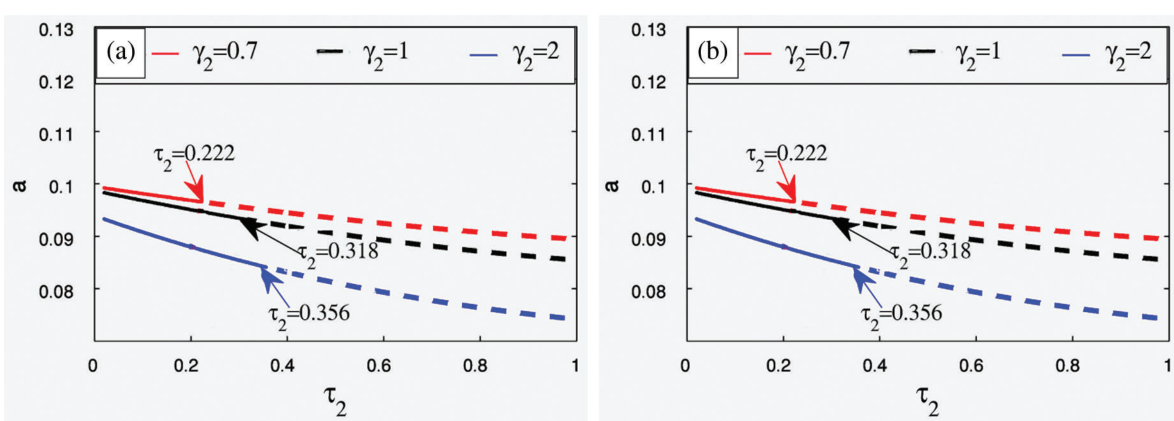

Figure 5: The response curve of the amplitude-delay τ_2 for (a) $\tau_1 = 0$ and (b) $\tau_1 = 0.03$

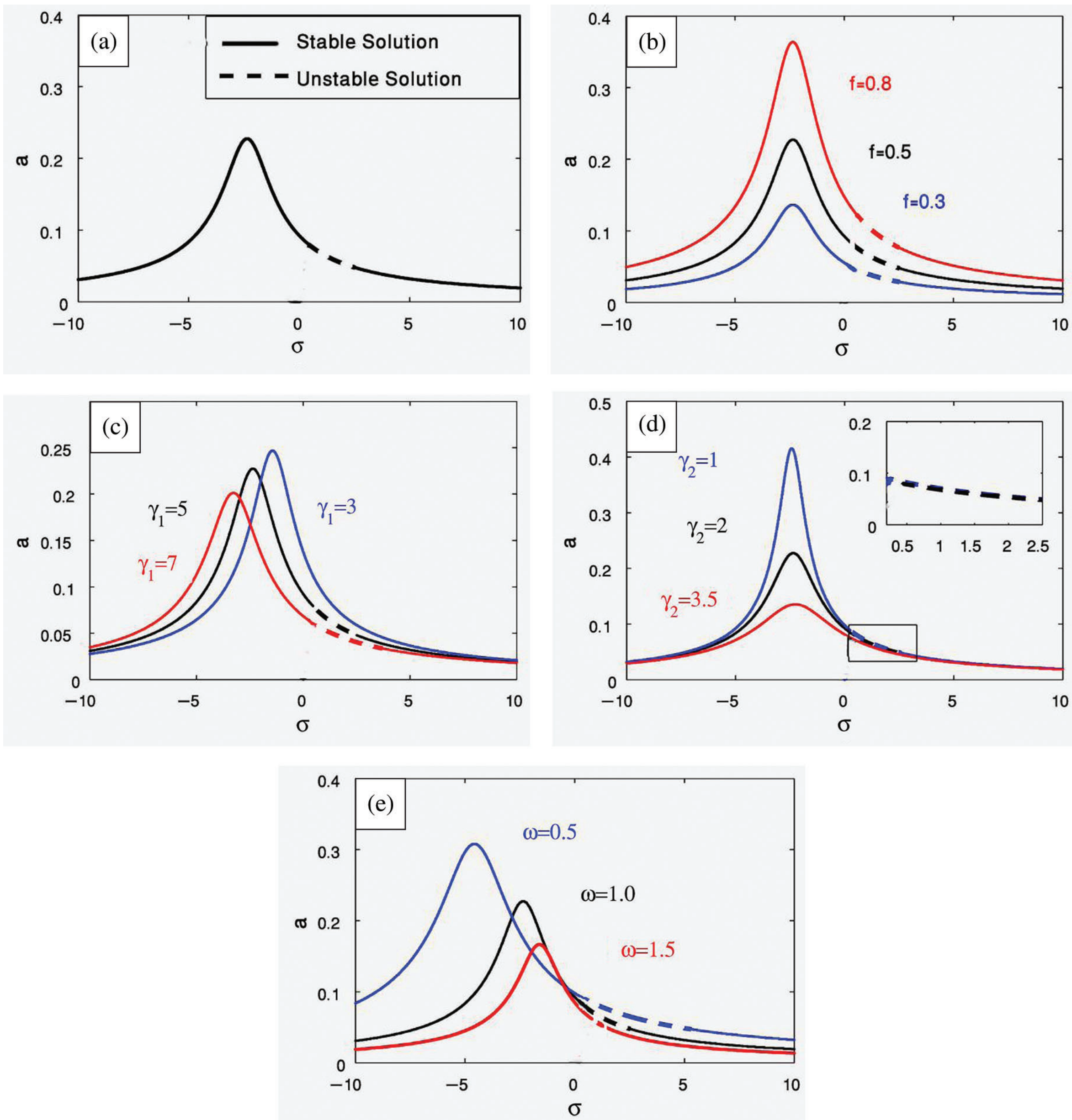

Figure 6: (a) The FRC of the controlled system. (b) The external force action. (c) The time delay displacement's feedback gain γ_1 action. (d) The time delay velocity's feedback gain γ_2 action. (e) The natural frequency ω action

consistent with Fig. 5b. For natural frequency ω, the main system's amplitude is monotonic decreasing function and shifted to right as shown in Fig. 6e.

Fig. 7 presents the response of the main system a against the external force f before and after control, from this figure we can see that, the effectiveness of the time delay control for suppression the vibrations of the main system. The Eqs. (24) and (25) solved analytically and presented graphically by (———) lines which be in agreement with the numerical solution of Eq. (1) as shown in Fig. 8. From Fig. 9, there is a

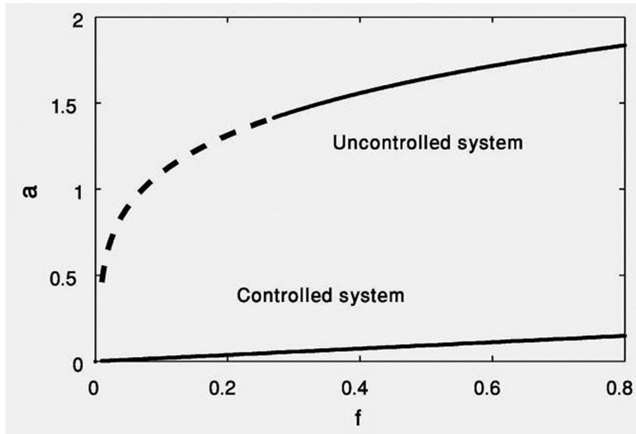

Figure 7: Response curve of force-amplitude of the system

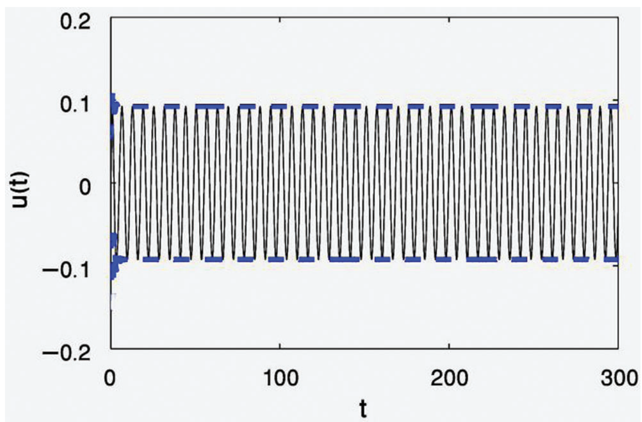

Figure 8: Comparison between the numerical solution (———) and the perturbation analysis (——————) for the controlled system

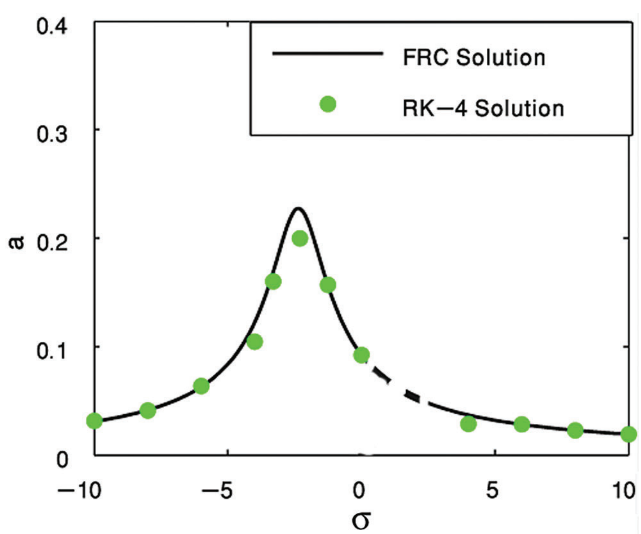

Figure 9: Comparison between the FRC Solution and RK-4 Solution

good agreement between the frequency response curves (FRC) which given by the sold line and the numerical solution of Eq. (1) using (RK-4) that marked by green circles.

5 Conclusion

Time delay control has been illustrated for the primary resonance case ($\Omega \cong \omega$) of the hybrid Rayleigh–van der Pol–Duffing oscillator. The solution of the nonlinear system from the first approximation is obtained applying the method of multiple scales. We success to reduce the vibrations of the hybrid Rayleigh–van der Pol–Duffing oscillator from 1.5 to 0.09 by using Time delay control.

The study divulged that:

1. For increasing the value of external excitation leads to increasing in the system amplitude.
2. The amplitude of the system is a monotonic decreasing function on the natural frequency ω and the time delay velocity's feedback gains γ_2.
3. The vibration suppression region increased for small values of the time delay displacement's feedback gains γ_1.
4. For $\tau_1 = 0$, the vibration suppression region increased for small values of γ_2 but for $\tau_1 = 0.03$, the vibration suppression region increased for large values of γ_2.
5. For the response curves, there is a good agreement between the FRC Solution and RK-4 Solution.

Funding Statement: The author(s) received no specific funding for this study.

Conflicts of Interest: The authors declare that they have no conflicts of interest to report regarding the present study.

References

1. Guckenheimer, J., Holmes, P., Slemrod, M. (1984). Nonlinear oscillations dynamical systems, and bifurcations of vector fields. *Journal of Applied Mechanics, 51(4),* 947. DOI 10.1115/1.3167759.
2. Lazzouni, S. A., Siewe, M. S., Kakmeni, F. M., Bowong, S. (2006). Slow flow solutions and chaos control in an electromagnetic seismometer system. *Chaos, Solitons & Fractals, 29(4),* 988–1001. DOI 10.1016/j.chaos.2005.08.061.
3. Siewe, M. S., Kakmeni, F. M., Bowong, S., Tchawoua, C. (2006). Non-linear response of a self-sustained electromechanical seismographs to fifth resonance excitations and chaos control. *Chaos, Solitons & Fractals, 29(2),* 431–445. DOI 10.1016/j.chaos.2005.08.210.
4. Siewe, M. S., Kakmeni, F. M., Tchawoua, C. (2004). Resonant oscillation and homoclinic bifurcation in a Φ^6-van der pol oscillator. *Chaos, Solitons & Fractals, 21(4),* 841–853. DOI 10.1016/j.chaos.2003.12.014.
5. Trueba, J. L., Baltanás, J. P., Sanjuán, M. A. (2003). A generalized perturbed pendulum. *Chaos, Solitons & Fractals, 15(5),* 911–924. DOI 10.1016/S0960-0779(02)00210-2.
6. Ueda, Y. (1979). Randomly transitional phenomena in the system governed by Duffing's equation. *Journal of Statistical Physics, 20(2),* 181–196. DOI 10.1007/BF01011512.
7. Wen, S., Shen, Y., Li, X., Yang, S. (2016). Dynamical analysis of Mathieu equation with two kinds of van der Pol fractional-order terms. *International Journal of Non-Linear Mechanics, 84,* 130–138. DOI 10.1016/j.ijnonlinmec.2016.05.001.
8. Huang, C. (2018). Multiple scales scheme for bifurcation in a delayed extended van der Pol oscillator. *Physica A: Statistical Mechanics and Its Applications, 490,* 643–652. DOI 10.1016/j.physa.2017.08.035.
9. Barron, M. A. (2016). Stability of a ring of coupled van der Pol oscillators with non-uniform distribution of the coupling parameter. *Journal of Applied Research and Technology, 14(1),* 62–66. DOI 10.1016/j.jart.2016.01.002.
10. Kimiaeifar, A., Saidi, A. R., Bagheri, G. H., Rahimpour, M., Domairry, D. G. (2009). Analytical solution for Van der Pol–Duffing oscillators. *Chaos, Solitons & Fractals, 42(5),* 2660–2666. DOI 10.1016/j.chaos.2009.03.145.

11. Soleman, S. M., Amer, Y. A. (2015). The time delayed feedback control to suppress the vibration of the autoparametric dynamical system. *Scientific Research and Essays, 10(15),* 489–500. DOI 10.5897/SRE2015.6208.
12. Cveticanin, L., El-Latif, G. A., El-Naggar, A. M., Ismail, G. M. (2008). Periodic solution of the generalized Rayleigh equation. *Journal of Sound and Vibration, 318(3),* 580–591. DOI 10.1016/j.jsv.2008.04.023.
13. Kumar, P., Narayanan, S., Gupta, S. (2016). Investigations on the bifurcation of a noisy Duffing–van der Pol oscillator. *Probabilistic Engineering Mechanics, 45,* 70–86. DOI 10.1016/j.probengmech.2016.03.003.
14. Kumar, P., Kumar, A., Erlicher, S. (2017). A modified hybrid Van der Pol–Duffing–Rayleigh oscillator for modelling the lateral walking force on a rigid floor. *Physica D: Nonlinear Phenomena, 358,* 1–14. DOI 10.1016/j.physd.2017.07.008.
15. Kumar, P., Kumar, A., Racic, V., Erlicher, S. (2018). Modelling vertical human walking forces using self-sustained oscillator. *Mechanical Systems and Signal Processing, 99,* 345–363. DOI 10.1016/j.ymssp.2017.06.014.
16. Saeed, N. A., El-Ganini, W. A., Eissa, M. (2013). Nonlinear time delay saturation-based controller for suppression of nonlinear beam vibrations. *Applied Mathematical Modelling, 37(20–21),* 8846–8864. DOI 10.1016/j.apm.2013.04.010.
17. Abdelhafez, H., Nassar, M. (2016). Effects of time delay on an active vibration control of a forced and self-excited nonlinear beam. *Nonlinear Dynamics, 86(1),* 137–151. DOI 10.1007/s11071-016-2877-z.
18. El-Ganaini, W. A., Kandil, A., Eissa, M., Kamel, M. (2016). Effects of delayed time active controller on the vibration of a nonlinear magnetic levitation system to multi excitations. *Journal of Vibration and Control, 22 (5),* 1257–1275. DOI 10.1177/1077546314536753.
19. Amer, Y. A., El-Sayed, A. T., Kotb, A. A. (2016). Nonlinear vibration and of the Duffing oscillator to parametric excitation with time delay feedback. *Nonlinear Dynamics, 85(4),* 2497–2505. DOI 10.1007/s11071-016-2840-z.
20. El-Sayed, A. T., Bauomy, H. S. (2014). Vibration control of helicopter blade flapping via time-delay absorber. *Meccanica, 49(3),* 587–600. DOI 10.1007/s11012-013-9813-9.
21. Xu, J., Chung, K. W., Zhao, Y. Y. (2010). Delayed saturation controller for vibration suppression in a stainless-steel beam. *Nonlinear Dynamics, 62(1–2),* 177–193. DOI 10.1007/s11071-010-9708-4.
22. Marinca, V., Herisanu, N. (2012). *Nonlinear dynamical systems in engineering: some approximate approaches*. USA: Springer Science & Business Media.
23. Nayfeh, A. H., Mook, D. T. (1979). *Nonlinear oscillations*. New York: Wiley.

Appendix

$$M_1 = -\frac{2\hat{\mu}\eta A^2}{3},\ M_2 = 0.25\hat{\mu}A^3(\mathrm{k} + 5\lambda\mathrm{A}\bar{\mathrm{A}}) + i(\beta+\delta)),\ M_3 = -2(\hat{\mu}\theta\omega^2A^4)e^{4i\omega T_0}$$

$$M_4 = -\frac{1}{12}(\hat{\mu}\lambda A^5),\ M_5 = \left(\frac{\hat{f}}{2(\omega^2-\Omega^2)}\right)$$

$$\begin{aligned}\xi = {} & 0.25\gamma_1^2\tau_1^2 + 0.25\gamma_2^2\tau_2^2\omega^2 + \omega^2 - 0.5\gamma_1\gamma_2\tau_1\tau_2\omega\sin(\omega\tau_1 - \omega\tau_2) \\ & + \gamma_1\tau_1\omega\sin(\omega\tau_1) - \gamma_2\tau_2\omega^2\cos(\omega\tau_2)\end{aligned}$$

$$\Gamma_1 = 0.3125\mu\lambda\omega^2(\gamma_1\tau_1\cos(\omega\tau_1) + \gamma_2\tau_2\omega\sin(\omega\tau_2))$$

$$\begin{aligned}\Gamma_2 = {} & -0.0625\gamma_1\tau_1\mu\omega^2(\beta+3\delta)\sin(\omega\tau_1) + 0.0625\gamma_2\tau_2\mu\omega^3(\beta+3\delta)\cos(\omega\tau_2) \\ & - 0.125\mu\omega^3(\beta+3\delta) + 0.375\mu k\omega^2(\gamma_1\tau_1\cos(\omega\tau_1) + \gamma_2\tau_2\omega\sin(\omega\tau_2))\end{aligned}$$

$$\Gamma_3 = \left(0.25\gamma_2^2\tau_2 + \mu\right)\omega^2 - 0.5\gamma_2\omega^2(1 + \mu\tau_2)\cos(\omega\tau_2) + 0.5\gamma_1\omega(1 + \mu\tau_1)sin(\omega\tau_1)$$
$$- 0.25\omega\gamma_1\gamma_2(\tau_1 + \tau_2)\sin(\omega\tau_1 - \omega\tau_2) + 0.25\gamma_1^2\tau_1$$

$$\Gamma_4 = 0.25\gamma_1\tau_1\lambda\omega^2 f, \quad \Gamma_5 = 0.25\gamma_2\tau_2\omega f, \quad \Gamma_6 = 0.5\omega f, \quad \Gamma_7 = 0.625\mu\lambda\omega^3 + 0.3125\mu\lambda\omega^2(\gamma_1\tau_1\sin(\omega\tau_1)$$
$$-\gamma_2\tau_2\omega\cos(\omega\tau_2))$$

$$\Gamma_8 = 0.0625\gamma_1\tau_1\mu\omega^2(\beta + 3\delta)\cos(\omega\tau_1) + 0.0625\gamma_2\tau_2\mu\omega^3(\beta + 3\delta)\sin(\omega\tau_2)$$
$$+ 0.75\mu k\omega^3 + 0.375\mu k\omega^2(\gamma_1\tau_1\sin(\omega\tau_1) - \gamma_2\tau_2\omega\cos(\omega\tau_2))$$

$$\Gamma_9 = 0.5\gamma_2\omega^2(1 - \mu\tau_2)\sin(\omega\tau_2) + 0.5\gamma_1\omega(1 - \mu\tau_1)\cos(\omega\tau_1)$$
$$+ 0.25\omega\gamma_1\gamma_2(\tau_1 - \tau_2)\cos(\omega\tau_1 - \omega\tau_2)$$

$$\Gamma_{10} = 0.25\gamma_1\tau_1 f, \quad \Gamma_{11} = 0.25\gamma_2\tau_2\omega f, \quad \Gamma_{12} = 0.5\omega f$$